Optical phase modulators using deformable waveguides actuated by micro-electro-mechanical systems

Wei-Chao Chiu,[1] Chun-Che Chang,[1] Jiun-Ming Wu,[1] Ming-Chang M. Lee,[1,*] and Jia-Min Shieh[2]

[1]*Institute of Photonics Technologies, National Tsing Hua University, HsinChu 300, Taiwan*

[2]*National Nano Device Laboratories, HsinChu 300, Taiwan*

**Corresponding author: mclee@ee.nthu.edu.tw*

Received January 18, 2011; revised February 24, 2011; accepted February 24, 2011;
posted February 25, 2011 (Doc. ID 141249); published March 18, 2011

An optical phase modulator is presented by using micro-electro-mechanical systems to actuate deformable silicon waveguides. Via mechanically stretching the waveguide length, the optical path is extended, resulting in a phase shift. The experimental results show that a phase shift of near 0.4π is achieved at 200 V for both TE- and TM-polarized waves by cascading six phase modulation units, agreeing well with the theoretical prediction. The power consumption is estimated to be smaller than 0.2 mW at 200 V, mainly resulting from the leakage current. © 2011 Optical Society of America

OCIS codes: 130.3120, 230.4685, 250.7360, 120.5060.

Integrated photonics for optical interconnects and optical signal processing have gained a lot of attention recently due to the large demands of distributed optical access networks and high-speed data transfer for supercomputers. Among the photonic devices, optical phase modulators are the key components for large-scale, complex photonic integrated circuits performing sophisticated optical functions such as switching, modulating, dynamic multiplexing, and demutiplexing [1,2]. The commonly used mechanisms for integrated photonic devices to achieve phase modulation rely on electro-optic, thermo-optic [3], or free-carrier dispersion [4]. Electro-optics is widely used for phase modulation. However, it is only applicable to some particular semiconductors or polymers. Thermo-optics is the easiest way to modulate optical phase. However, slow response time, thermal crosstalk, and high-energy consumption are still issues. Free-carrier dispersion has been demonstrated with a modulation speed of tens of gigabit per second as well as low power consumption based on the metal-oxide semiconductor [5], *p-i-n* or *p-n* diode structures [6]. Nevertheless, free-carrier absorption accompanying free-carrier dispersion can induce extra amplitude modulation, which could impair optical interference as well.

Integrating micro-electro-mechanical systems (MEMS) with silicon waveguides can be an applicable approach for phase modulation without introducing optical absorption. Fuchs *et al.* [7] used movable micromirrors to alter the free-space optical path of wave reflection, and Ikeda *et al.* [8] utilized movable waveguides in a directional coupler configuration to achieve an equivalent variable optical path. However, pure linear motion of optical components actuated by micrometer comb-drive is critical [9]. Previously, a compact, tunable optical microresonator with variable coupling ratio based on MEMS-actuated deformable silicon waveguides was reported and demonstrated for a variety of optical functions [10,11]. In this Letter, we further give a comprehensive study on the phase change with respect to waveguide deformation [12] and present a realization of phase modulators.

A deformable waveguide actuated by electrostatic force is illustrated in Fig. 1(a). The waveguide, made on silicon-on-insulator, is released by selectively removing the bottom SiO_2. Upon applying bias, the waveguide is deformed and pulled toward the electrode, causing the optical path to be extended. Figure 1(b) shows the micrograph of a fabricated phase modulation unit at $V = 0$ V. Directly stretching the waveguide physical length is very efficient to induce a phase shift for a guided wave but not to introduce much amplitude variation. In this study, the suspended waveguide is designed to be 150 μm long, 5 μm high, and 0.3 μm wide. The initial gap spacing between the waveguide and electrode is 6 μm.

To quantitatively analyze waveguide stretching, a finite element simulator (COMSOL Multiphysics) is used to model waveguide deformation at different bias voltages. The results are shown in Fig. 2(a). By examining the deformed waveguide shape before pull-in, which occurs at the bias of 527.63 V, the waveguide extension length and the corresponding phase shift of the TM_{00} guided mode at 1550 nm are calculated and plotted in Fig. 2(b). A 0.1π phase shift is achieved at a bias of 240 V. A large dynamic range of phase modulation can be accomplished if multiple waveguide actuators are cascaded. Stress in deformed waveguides could also contribute to a phase shift due to the photoelastic effect [13]. The stress-induced index variation of refraction can be modeled as follows:

$$\begin{aligned}\Delta n_x &= n_x - n_0 = -C_1\sigma_x - C_2(\sigma_y + \sigma_z),\\ \Delta n_y &= n_y - n_0 = -C_1\sigma_y - C_2(\sigma_x + \sigma_z),\\ \Delta n_z &= n_z - n_0 = -C_1\sigma_z - C_2(\sigma_x + \sigma_y),\end{aligned} \tag{1}$$

where σ_x, σ_y, and σ_z are the principal stress tensor components along the x, y, and z axes, respectively. n_0 is the material refractive index without stress. C_1 and C_2 are

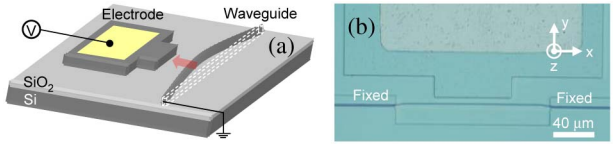

Fig. 1. (Color online) (a) Schematic of a MEMS-actuated phase modulation unit consisting of a deformable waveguide and an electrode, (b) top-view micrograph of a fabricated phase modulation unit.

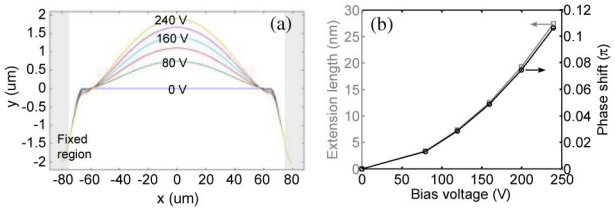

Fig. 2. (Color online) (a) Simulated waveguide deformation at different bias voltages, (b) calculated waveguide extension and the corresponding phase shift as functions of bias voltage.

the stress-optical coefficients, relating to Young's modulus E, Poisson's ratio ν, and the photoelastic tensor elements p_{11} and p_{12} given by

$$C_1 = \frac{n_0^3}{2E}(p_{11} - 2\nu p_{12}), \qquad C_2 = \frac{n_0^3}{2E}(-\nu p_{11} + (\nu - 1)p_{12}). \tag{2}$$

Table 1 summarizes the material parameters used for analyzing the photoelastic effect of the deformable waveguide. Although the photoelastic tensor elements p_{ij} were measured at 1150 nm[13], the wavelength dependency is relatively weak. By applying Eqs. (1) and (2) into the mechanical simulation model, the stress-induced Δn is calculated to be about the magnitude of $\pm 1 \times 10^{-4}$ in both Δn_z and Δn_y at 240 V. The accumulated phase shifts due to the photoelastics are thus estimated to be -0.0017π and -0.001π for the TE_{00} and TM_{00} guided modes, respectively. These values are about 2 orders of magnitude smaller than the phase shift caused by waveguide elongation, indicating that the photoelastic effect can be neglected in this case.

The optical loss created by waveguide actuation was examined by measuring optical transmission of a deformed waveguide. A broadband amplified spontaneous emission from 1520 to 1570 nm was launched into one end of the waveguide, and the transmitted power was measured at the other end. Since high-order guided modes could be excited in the waveguide, the input wave is properly aligned to primarily couple to the fundamental mode for better device characterization. The propagation losses of the suspended waveguide were measured to be 6.42 and 4.11 dB/cm for the TE- and TM-polarized waves, respectively. At a bias of 200 V, the optical losses were merely increased by 0.063 and 0.053 dB for the TE- and TM-guided waves, showing that the waveguide transmittance is barely influenced by the mechanical motion. A slightly larger loss for the TE polarization state could be attributed to larger mode overlapping with the inhomogeneous surface roughness.

To experimentally investigate the phase shift induced by MEMS actuation, a monolithically integrated Mach–Zehnder interferometer (MZI) is used for converting the phase shift to amplitude modulation. The device

Table 1. Material Parameters of Silicon

Young's Modulus (E) GPa	Poisson's Ratio ν	Refractive Index n_0	Photoelastic Tensor Elements p_{11}	p_{12}
180	0.29	3.45	−0.101	0.0094

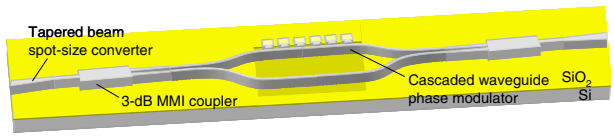

Fig. 3. (Color online) Schematic of a MEMS-actuated MZI.

structure is shown in Fig. 3. Six units of deformable waveguide are employed at one arm of the MZI. An adiabatic beam spot-size converter is used to convert an optical mode smoothly from a fiber to the silicon waveguide for reducing the coupling loss. Two 3 dB multimode interference (MMI) couplers are integrated to split and combine light waves. Details of the device design and fabrication processes were reported in [12]. A linearly polarized, 10 mW tunable laser at central wavelength of 1550 nm was used to characterize the phase shift of waveguide deformation. To improve waveguide-fiber coupling, spherical polarization-maintaining lensed fibers with a spot size of 8.5 μm were aligned to the two ends of the waveguide. A direct current (DC) bias voltage was applied to the electrodes, and the suspended waveguides were electrically grounded. The breakdown voltage of the electrode was measured to be 250 V under DC bias conditions. The output power of MZI was measured by a photodetector and then converted to the phase shift according to the equation given by $\phi_s = \cos^{-1}\left[\frac{(1+r)(1-R)+2\sqrt{r}}{2R\sqrt{r}}\right]$ and $R = \frac{P_0}{P_{\text{out}}}$, where ϕ_s is the phase shift in radian for one arm, r is the MMI split ratio, and P_0 and P_{out} are the output optical powers before and after actuation, respectively. Because the power imbalance of the 3 dB MMI coupler was measured to be within 0.1 dB around the wavelength of 1550 nm, r is assumed to be 1 here. The optical power measurement errors caused by fiber misalignment were within $\pm 0.06\,\mu$W, which yields the phase measurement errors within -0.03π and $+0.04\pi$. Figure 4(a) shows the measured polarization-dependent phase shifts at different bias voltages. The phase shift increases gradually with the applied voltage and reaches to near 0.4π at 200 V for both TE- and TM-polarized waves. However, the TE wave generally shows a slightly smaller value. The deviated phase shift is within 0.1π, which could be caused by polarization mode dispersion where the effective refractive indices for the TE_{00} and TM_{00} guided modes are calculated to be 2.44 and 3.0, respectively. By tuning the wavelength to 1540 and 1555 nm for the TM-polarized wave, the

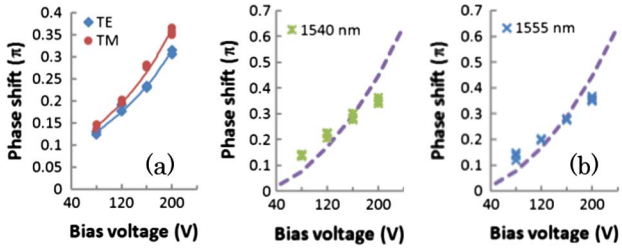

Fig. 4. (Color online) Experimental results on phase modulation. (a) Measured phase shifts as functions of bias voltages for the TE- and TM-polarized waves, (b) measured phase shifts at the wavelengths of 1540 and 1555 nm for the TM-polarized wave. The theoretical curves (dashed line) are calculated by the finite element method.

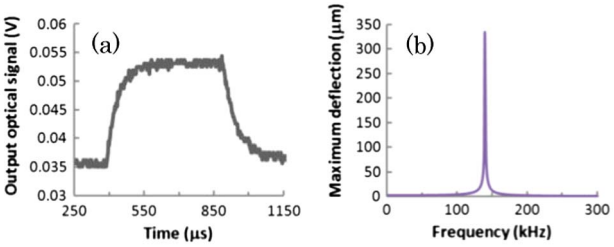

Fig. 5. (Color online) (a) Measured dynamic response of the modulated optical signal, (b) simulated frequency response of a 150-μm-long suspended silicon waveguide.

measured phase shifts are presented in Fig. 4(b). For either wavelength, the phase shifts with respect to the bias voltages are very similar, showing the device is not wavelength sensitive. The experimental data at 200 V exhibit a slightly larger deviation near -0.1π from the simulation results, which could be attributed to multimode excitation in the deformed silicon waveguides where the high-order guided modes experience lower effective refractive indices.

To verify the MEMS actuation speed, a 1 kHz square-wave signal with a peak-to-peak voltage of 240 V was applied to the electrodes. The input light was controlled to be TM-polarized. The modulated optical signal was measured by a photodetector and shows a dynamic on–off extinction ratio of 2 dB. A much higher extinction ratio can be accomplished by cascading more phase modulation units to reach a π phase shift. Moreover, the rise time (10%–90%) of the modulated signal was estimated to be near 88 μs according to the dynamic response shown in Fig. 5(a). The natural frequency of vibration for this 150-μm-long suspended silicon waveguide is in fact simulated to be 139 kHz, as shown in Fig. 5(b). To reduce the bias voltage and increase the actuation speed, an optimal design on the waveguide length and the gap spacing between the waveguide and electrode is essential for practical applications. Cascading more phase modulation units is also useful to decrease the bias voltage but keep the total phase shift unchanged. Static power dissipation of this modulation unit mainly results from the leakage current, which is smaller than 1 μA, corresponding to the power consumption of 0.2 mW at 200 V.

In summary, we have demonstrated an integrated optical phase modulator using MEMS-actuated deformable silicon waveguides. The optical phase shift is controlled through mechanically stretching the waveguide length. Based on this mechanism, a 0.06π phase shift was achieved by actuating a single waveguide at 200 V; meanwhile, the amplitude variation during the mechanical actuation was shown to be only 0.063 dB for both TE- and TM-polarized waves. By cascading multiple waveguide actuators, the phase shift accumulates and could result in a large dynamic range. To verify this idea, a numerical analysis was developed by the finite element method, and the simulation results are in good agreement with the experimental data. Overall, this MEMS-actuated deformable waveguide can be used as a phase modulation unit with less amplitude variation and low power consumption.

The work is supported by the National Science Council of Taiwan (NSCT) (NSC98-2622-E-007-002-CC1, 98-2221-E-007-022-MY3) and National Nano Device Laboratories (NDL98-C02M3C-040) in Taiwan.

References

1. B. Jalali and S. Fathpour, J. Lightwave Technol. **24**, 4600 (2006).
2. R. Won and M. Paniccia, Nat. Photon. **4**, 498 (2010).
3. G. Cocorullo and I. Rendina, Electron. Lett. **28**, 83 (1992).
4. R. A. Soref and B. R. Bennett, IEEE J. Quantum Electron. **23**, 123 (1987).
5. A. Liu, R. Jones, L. Liao, D. Samara-Rubio, D. Rubin, O. Cohen, R. Nicolaescu, and M. Paniccia, Nature **427**, 615 (2004).
6. M. Lipson, J. Lightwave Technol. **23**, 4222 (2005).
7. D. T. Fuchs, H. B. Chan, H. R. Stuart, F. Baumann, D. Greywall, M. E. Simon, and A. Wong-Foy, Electron. Lett. **40**, 142 (2004).
8. T. Ikeda, K. Takahashi, Y. Kanamori, and K. Hane, Opt. Express **18**, 7031 (2010).
9. C. Shiang-Woei, L. Yunn-Shiuan, and C. Jeng-Tzong, J. Microelectromech. Syst. **14**, 305 (2005).
10. M. C. M. Lee and M. C. Wu, Opt. Lett. **31**, 2444 (2006).
11. J. Yao and M. C. Wu, Opt. Lett. **34**, 2557 (2009).
12. C. C. Chang, W. C. Chiu, J. M. Wu, M. C. M. Lee, and J. M. Shieh, in *2010 International Conference on Optical MEMS and Nanophotonics (OPT MEMS)*, (IEEE, 2010), pp. 99–100.
13. W. N. Ye, D. X. Xu, S. Janz, P. Cheben, M. J. Picard, B. Lamontagne, and N. G. Tarr, J. Lightwave Technol. **23**, 1308 (2005).